의학박사 학위논문

A Rat Model of Chronic Syringomyelia by Epidural Compression of the Lumbar Spinal Cord

요추부 척수의 경막외 압박에 의한 만성 척수공동증 랫드 모델

2014 년 2 월

서울대학교 대학원
의학과 뇌신경과학 박사과정
이 지 연

A Rat Model of Chronic Syringomyelia by Epidural Compression of the Lumbar Spinal Cord

2014년

이 지 현

의학박사 학위논문

A Rat Model of Chronic Syringomyelia by Epidural Compression of the Lumbar Spinal Cord

요추부 척수의 경막외 압박에 의한 만성 척수공동증 랫드 모델

2014 년 2 월

서울대학교 대학원
의학과 뇌신경과학 박사과정
이 지 연

A thesis of the Degree of Doctor of Philosophy

요추부 척수의 경막외 압박에 의한 만성 척수공동증 랫드 모델

A Rat Model of Chronic Syringomyelia by Epidural Compression of the Lumbar Spinal Cord

February 2014

The Department of Neuroscience,
Seoul National University
College of Medicine
Ji Yeoun Lee

요추부 척수의 경막외 압박에 의한 만성 척수공동증 랫드 모델

지도교수 백 선 하

이 논문을 의학박사 학위논문으로 제출함.

2013년 10월

서울대학교 대학원

의학과 뇌신경과학 전공

이 지 연

이지연의 의학박사 학위논문을 인준함.

2013년 12월

위 원 장 김 기 중

부위원장 백 선 하

위 원 왕 규 창

위 원 천 정 은

위 원 심 기 범

A Rat Model of Chronic Syringomyelia by Epidural Compression of the Lumbar Spinal Cord

by
Ji Yeoun Lee

A thesis submitted to the Department of Neuroscience in partial fulfillment of the requirements for the Degree of Doctor of Philosophy in Medical Science (Neuroscience) at Seoul National University College of Medicine

December 2013

Approved by Thesis Committee:

Professor Ki Joong Kim Chairman

Professor Sun Ha Paek Vice chairman

Professor Kyu-Chang Wang

Professor Jung-Eun Cheon

Professor Ki-Bum Sim

ABSTRACT

Introduction

There has been no established animal model of syringomyelia associated with lumbosacral spinal lipoma. The research on pathophysiology of syringomyelia has been focused on Chiari malformation, trauma, and inflammation. To help understand the underlying pathophysiology of syringomyelia associated with occult spinal dysraphism, a novel animal model for the syringomyelia by chronic mechanical compression of the lumbar spinal cord was attempted.

Methods

The model was made by epidural injection of highly-concentrated paste-like kaolin after partial laminectomy of L1 and L5 level. Behavioral outcome in terms of motor (Basso-Beattie-Bresnahan score) and urinary function was assessed until 12 weeks. Magnetic resonance images (MRI) were used to confirm the formation of syrinx and its extent, and various immunohistochemistry (IHC) studies including GFAP, ED-1, CC1, NeuN, caspase-3, and LFB were done to evaluate the degrees of inflammatory reaction, demyelination, and cell death.

Results

By 12 weeks after the operation, syringomyelia formation was confirmed in 85% of the rats (34 out of 40) on H & E staining and MRI. Motor deficit of

variable degree was seen immediately after the procedure in 28% (11 out of 40) of the rats. In 13 rats (33%), lower urinary tract dysfunction was seen. Motor deficit improved until 5 weeks after the operation, whereas majority of the urinary deficit improved in the first 2 weeks. There was delayed mortality of 13% (5 out of 40), later than 1 month after the operation and 3 of the 5 died from new onset urinary dysfunction. Serial MRI (n = 1) revealed that prominent syringomyelia was visible 2 months after the operation, and that the syrinx cavities were located proximal to the compression. At 12 weeks after the operation, IHC showed no increase of inflammation or demyelination in these models, compared to sham operation cases.

Conclusions

A novel experimental model for the syringomyelia by epidural compression of the lumbar spinal cord has been established. It will serve as an important research tool to elucidate the pathogenesis of this type of syringomyelia, and the CSF hydrodynamics of the lumbar spinal cord.

Keywords: syringomyelia, lumbar spinal cord, epidural compression, occult spinal dysraphism,

Student number: 2011-30612

CONTENTS

LIST OF FIGURES

LIST OF TABLES

LIST OF ABBREVIATIONS

axial (axi), Basso-Beattie-Bresnahan (BBB), central nervous system (CNS), cerebrospinal fluid (CSF), echo time (TE), field of view (FOV), flip angle (FA), hematoxylin and eosin (H & E), immunohistochemistry (IHC), luxol fast blue (LFB), magnetic resonance imaging (MRI), phosphate buffered saline (PBS), repetition time (TR), sagittal (sag), slice thickness (TH), spinal cord injury (SCI), standard deviation (SD), volume of interest (VOI)

INTRODUCTION

Syringomyelia is a fluid-filled cavity of the spinal cord or the central canal. There are different causes of syringomyelia, such as Chiari malformation, arachnoiditis, and trauma, and although the syringes have similar appearance, the underlying mechanisms vary (1). More importantly, therapeutic strategy differs according to the underlying disease. Therefore, elucidation of the pathogenesis of syringomyelia and the associated condition is not only a matter of academic curiosity but is of clinical importance.

Syringomyelia in association with occult spinal dysraphism such as lumbosacral lipoma or tethered cord syndrome has been well recognized and documented, especially with the wide use of magnetic resonance imaging (MRI) as a diagnostic tool for spinal dysraphisms (Figure 1). Various clinical characteristics of this type of syringomyelia have been considered as distinct from those caused by Chiari malformation, trauma or arachnoiditis (2)(3). Also, there has long been controversy regarding its clinical management, whether direct manipulation of the syrinx through syringotomy is necessary.

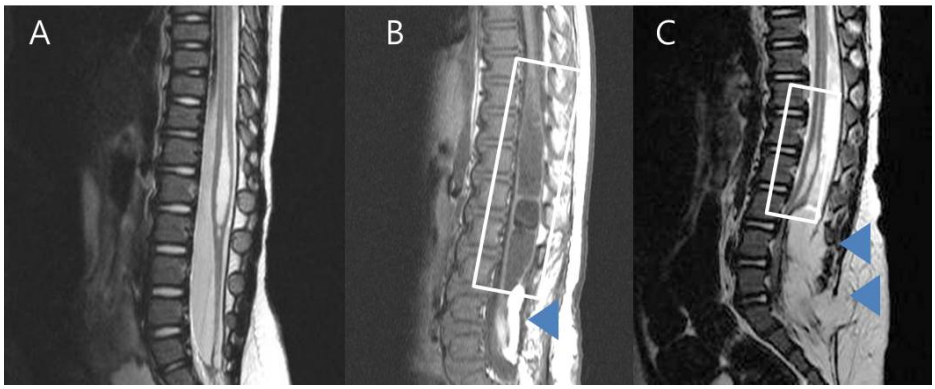

Figure 1. Syringomyelia associated with occult spinal dysraphism

(A) Sagittal T2WI show syringomyelia caused by simple tethered cord. (B) Sagittal T1WI show dorsal type lumbosacral lipoma depicted with arrow head, and syringomyelia in white box. (C) Transitional type lumbosacral lipoma depicted with arrow heads, and syringomyelia in white box on sagittal T2WI.

We have recently reviewed a fairly large group of occult spinal dysraphism patients with preoperative syringomyelia aiming to resolve the argument regarding its clinical management strategy (4). The results showed that untethering alone, without direct manipulation of the syringomyelia, may be appropriate as the management of these lesions. Apart from the answer to the main question of the study, some patients with a transient increase in the syrinx index during the initial postoperative period were noted, and surprisingly these may be observed without additional surgery if patients are symptomatically stable. This additional observation was important because usually surgeons would be frightened of retethering and feel urged to reoperate, on encountering an increase in syringomyelia. Such unexplained clinical phenomenon tempted the basic search on syringomyelia associated with occult spinal dysraphism.

One of the most crucial experimental tools to study the pathogenesis of a disease is an appropriate animal model resembling its core features. Active research on syringomyelia has provided a wide collection of animal models. Conventional animal models of syringomyelia, usually to study those related with Chiari malformation, were established by dilatation of the central canal or extra canalicular cavity (5-12). Other approaches have used injections of excitotoxic amino acids to reproduce the excitotoxic component of syringomyelia (12, 13). Animal models of posttraumatic syringomyelia have been established through various spinal cord injuries (SCI: weight-drop or clip compression injury) (11, 14, 15). Based on the results of research with animal models, many hypotheses have been drawn regarding the pathogenesis of

these syringomyelias. However, laboratory research on syringomyelia associated with occult spinal dysraphism has been limited and there is lack of an animal model.

Therefore, the present study aimed to develop a new animal model of syringomyelia by epidural compression of the lumbar spinal cord, resembling the mass effect of lumbosacral lipoma. Various attempts to induce chronic, noninflammatory compression of the spinal cord were made. The established model was evaluated in detail using neurobehavioral assessment, MRI, and immunohistochemistry (IHC).

Pilot study

In order to establish a novel animal model of syringomyelia by recapitulating chronic compression of the lumbar spinal cord, several factors had to be figured out. First, as for the compressing material, Gelfoam (Pfeizer, MI, USA; n = 3), adhesive glue (Okong, Incheon, Korea; n = 3), and kaolin (Sigma-Aldrich, MO, USA; n = 3) were attempted. Neither gelfoam nor adhesive glue was suitable as compressing material, because of the soft texture and possibility of absorption over time. Kaolin has been a material used historically for syringomyelia models, as a foreign body injected into the subpial or parenchymal space in low concentrations (1 ~ 10 mg / 1 ml) to induce inflammatory responses. For the present model, 1000 mg of kaolin was mixed with 1 ml of saline giving a semi-solid texture. The saline-mixed kaolin would dry into solid form after 1 hour. Kaolin mixed with saline in high

concentration provided enough viscosity to be injected into the epidural space even through a small laminectomy site.

Second, the mode of compression was to be decided. Initially, total laminectomy was performed in the entire lumbar region, from L1 to L5, and the compression material was put on the dorsal surface of dura and wound was closed (n = 3). However, the steadiness of compression could not be assured even after muscle and skin closure. Therefore, partial laminectomies at L1 (the injection entrance) and L5 were performed, leaving the posterior elements of the spine at L2, L3, L4 intact (n = 3) to work as a lid to provide consistent compression after injection (Figure 2).

Third, the duration of compression had to be decided. Although the modes of action were different, previous models were considered and 4 weeks (n = 8) and 6 weeks (n = 8) were attempted. However, none of the animals at 4 and 6 weeks developed syringomyelia as confirmed by tissue sections. Then a longer period of 12 week (n = 8) time point was chosen, and majority of the animals showed evidence of syringomyelia. The scheme of pilot study has been summarized in Figure 3.

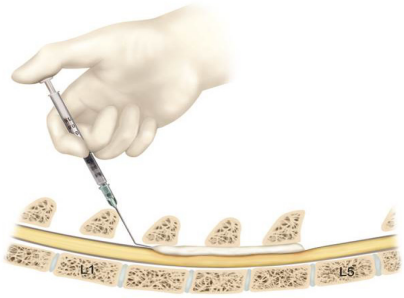

Figure 2. Medical illustration of epidural injection

The key step of the experiment, epidural injection of kaolin, is done using a 1 ml 26-gauge syringe with the tip bent through the L1 laminectomy site in the caudal direction.

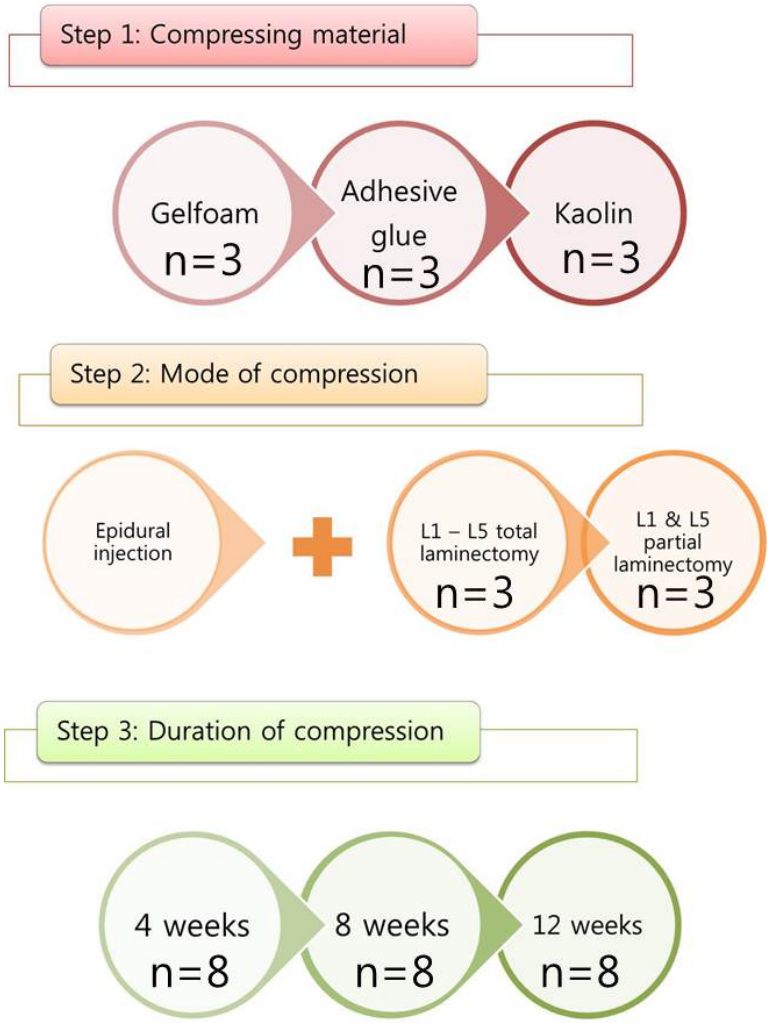

Figure 3. Diagram summary of pilot studies

Three aspects of the experimental procedure had to be decided to establish a successful animal model through pilot study. First, gelfoam, adhesive glue, and highly viscous kaolin were tried as candidate compressing materials (top row: step 1). The most effective method to achieve epidural compression had to be decided between total laminectomy of L1 to L5 level and partial laminectomy of L1 and L5 laminae (middle row: step 2). The duration of the compression had to be chosen, and 4, 8, 12 weeks were attempted (bottom row: step 3)

MATERIALS AND METHODS

1. Animals

Male Sprague-Dawley rats (6 weeks of age, weight: 175 to 200 g) were obtained from the Preclinical Research Center of the Clinical Research Institute of Seoul National University Hospital. The animals were kept in temperature-controlled rooms with a 12 hour light and 12 hour dark photoperiod, and were fed with standard rat food and water available freely. All procedures were approved by the Institutional Animal Care and Use Committee of Seoul National University Hospital (IACUC NO.12-2005-006-9).

2. Experimental procedure

Rats (n = 50) were anesthetized using ketamine (75 mg/kg, i.p.) and xylazine (10 mg/kg, i.p.). With the animal in prone position, midline skin incision was made in the lower thoracic to sacral level. After splitting the paravertebral muscles, partial laminectomies were performed at L1 and L5 level, leaving the entire laminae of L2-L4 intact. Paste-like kaolin (concentration: 1000 mg / 1 ml, amount: 0.01 ~ 0.02 ml) was injected in the epidural space using a 26-gauge needle in the caudal direction from the laminectomy site of L1 until the paste material squeezed out of the L5 laminectomy site. Control group animals (n = 5) were given sham surgeries by injecting saline after L1, L5 partial laminectomies in the identical way. After suturing of all wounds, the animals were allowed to recover under

heated lamps. After surgery, 0.1 ml meloxicam was administered for analgesia, and gentamycin was given as a prophylactic antibiotic. Manual palpation and compression of bladder was done for the animals, 3 times daily until no retention of urine was noticeable. The experimental procedure is summarized in Figure 4.

A

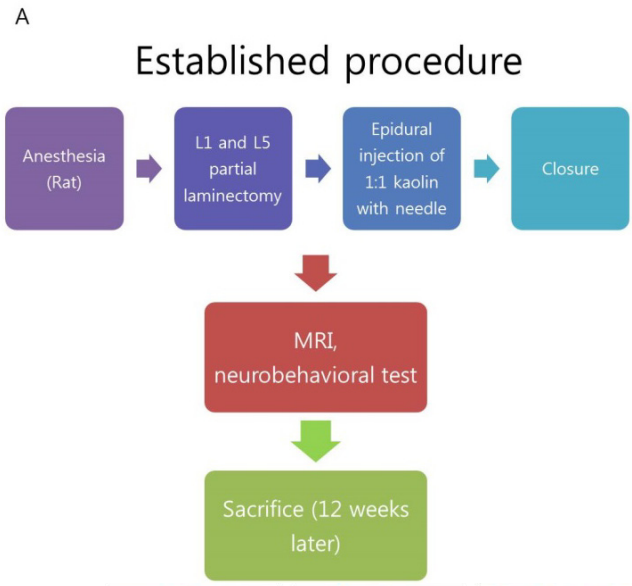
Established procedure
Anesthesia (Rat)
L1 and L5 partial laminectomy
Epidural injection of 1:1 kaolin with needle
Closure
MRI, neurobehavioral test
Sacrifice (12 weeks later)

B

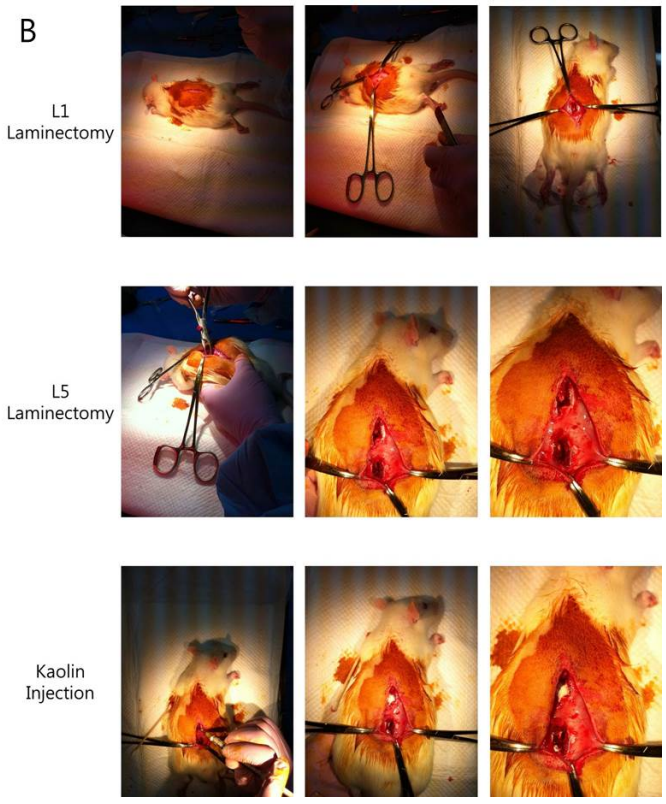
L1 Laminectomy
L5 Laminectomy
Kaolin Injection

Figure 4. Flow diagram and gross photographs of the established surgical procedure

Epidural compression was induced by injection of high-concentration kaolin into the epidural space after partial laminectomy of the L1 and L5 laminae. The model is maintained for 12 weeks before sacrifice.

(A) flow diagram, (B) gross photographs of the laminectomies and kaolin injection

3. In vivo *neurobehavioral evaluation*

The motor power of the lower limbs was evaluated using Basso-Beattie-Bresnahan (BBB) hindlimb locomotor test (16). BBB test is a widely used, reliable method to measure the hindlimb recovery of rats after various spinal cord injuries. Briefly, on a scale of 0 to 21, the following attributes were observed and scored: the movement of 3 joints of the hindlimb (scores 0 – 7); toe clearance, paw position, and forelimb-hindlimb coordination (scores 8 – 13); trunk stability, tail position(scores 14 – 21). Neurological assessment was performed every 2 days for the first week, then every week until the end of the study.

The functional status of the bladder was simply classified as urinary dysfunction or normal urinary function. The rats were assessed daily and urinary dysfunction was defined as when manual compression of the bladder was needed to completely empty the bladder.

4. MRI

Rats (n = 7) underwent MRI scans 3 months after operation. For 1 rat, serial images at 1 month, 2 months and 3 months were taken. For the MRI scan, rats were anesthetized with 1.5% isoflurane in room air. Respiration and temperature of the animals were monitored throughout the MRI session.

All MRI data were acquired by using a 9.4 T animal MR scanner (Agilent 9.4T/160AS; Agilent Technologies, CA, USA) with a volume coil for both RF transmission and signal reception (Agilent Technologies). Rats were positioned prone in the handling system. Following a global shimming over

the entire animal body, scout images were acquired in all 3 directions using a gradient echo sequence with the following imaging parameters; repetition time (TR) / echo time (TE) = 26 / 2.62 msec, flip angle (FA) = 30°, number of slices = 5, no interslice gap, slice thickness (TH) = 2 mm, field of view (FOV) = 70 × 70 mm^2, matrix size = 128 × 128, receiver bandwidth = 50 kHz, and 1 signal average.

Based on the scout image, a volume of interest (VOI) was defined followed by automated, local shimming thereof. Finally, T2-weighted images of the VOI were acquired in sagittal (sag) and/or axial (axi) planes by using a fat-saturated, respiratory-gated, multiple spin echo sequence. The imaging parameters were: TR / TE = 2000 / 13, 26, 39, 52, 65 msec, FA = 90° / 180°, number of slices = 10 (sag) and 12 (axi), interslice gap = 0 mm (sag) and 4.5-6 mm (axi), TH = 1 mm (sag) and 1.5 mm (axi), FOV = 90 × 55 mm^2 (sag) and 55 × 65 mm^2 (axi), matrix size = 256 × 192, receiver bandwidth = 50 kHz, and 2 signal averages.

5. Histopathology

All animals were sacrificed 12 weeks after the operation for histological analysis. Rats were given a lethal dose of thiopental sodium (200 mg / kg, i.p.; Sigma) and perfused with 4% paraformaldehyde solution in 0.1M phosphate buffer. Spinal cords were harvested and immersed in 4% paraformaldehyde solution for 24 h. After fixation, the tissues were serially immersed in 10%, 20% and 30% sucrose solution for dehydration. The specimens were embedded in paraffin using standard procedures. Histological spinal cord sections were cut

in the axial plane at 4 μm thickness and stained with hematoxylin and eosin (H&E) and luxol fast blue (LFB).

After H&E staining, the sagittal and axial sections were used to evaluate the morphology of the central canal in terms of size and shape in the entire lumbar cord and parts of thoracic cord. The central canal – spinal cord ratio was measured at where the section of widest central canal observed (Figure 5).

IHC studies were done (kaolin injected animals = 13, sham-operated controls = 2) to evaluate the degree of inflammation and demyelination. After 3 rinses in phosphate buffered saline (PBS), sections were blocked in normal goat serum for 30 minutes and washed in PBS. Then, the sections were incubated overnight with the primary antibody as following: mouse-monoclonal GFAP (1:300 dilution; Sigma) for reactive astrocytes, mouse-monoclonal ED-1 (1:200 dilution; Millipore, MA, USA) for macrophages or microglia, mouse-monoclonal CC1 (1:300 dilution; Novus Biological, CO, USA) for oligodendrocyte, mouse-monoclonal NeuN (1:300 dilution; Millipore) for neurons, and rabbit-polyclonal caspase-3 (1:300 dilution; Sigma) for apoptosis. Primary antibodies were diluted in PBS containing 1% normal goat serum. After rinsing with PBS, sections were incubated for 1 hour at room temperature with biotinylated anti-mouse or anti-rabbit IgG antibodies (Vector, CA, USA) diluted in 1:1,000. The secondary antibodies were detected using an avidin-biotin complex and visualized using diaminobenzidine (Sigma). The sections were washed in PBS for 3 times. The slides were analyzed using light microscopy and compared with sham-operated control samples.

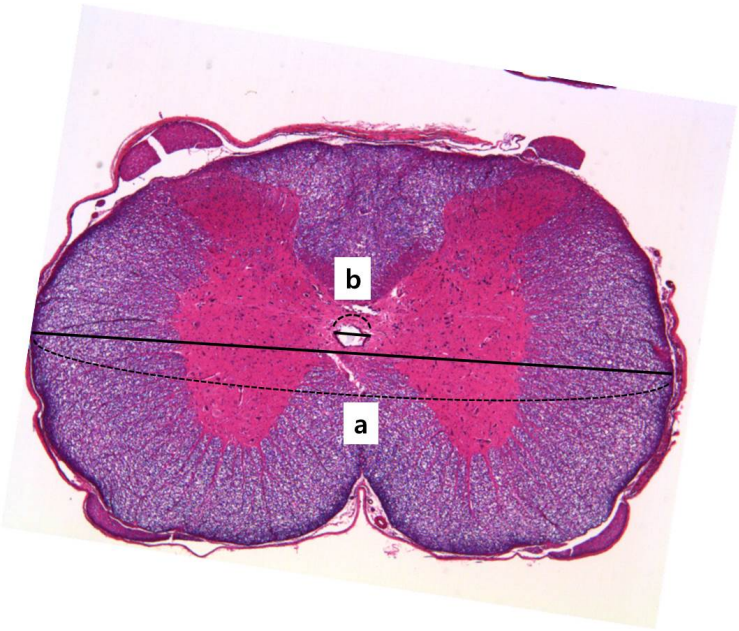

Figure 5. Central canal – spinal cord diameter ratio

Central canal – spinal cord ratio defined as the cross-sectional syringeal diameter calculated as a percentage of the spinal cord diameter ratio at the level of the largest cyst diameter

RESULTS

The early mortality of the model was fairly high (20%). Ten out of the 50 rats died or was sacrificed during the first 5 days of operation despite analgesics and antibiotics treatment. Poor recovery from anesthesia, operative bleeding, and severe urinary retention (full bladder with turbid or bloody urine) were probable reasons. Two animals showed seizure and autotomy, so they had to be sacrificed in the immediate postoperative period.

Five rats died during the subacute or delayed postoperative period. The cause of death for 3 of these was suspected to be urinary tract infection, either due to persistent or new onset urinary retention.

Thirty-four rats were confirmed to show syringomyelia on histology and/or MRI, resulting in a success rate of 68% (34 / 50). Excluding the 10 early mortality cases, this model succeeded in syringomyelia formation in 85% of the animals.

Neurobehavioral Outcome

Behavioral test was done for 40 rats, excluding the 10 rats that died in the early postoperative period. Eleven out of 40 rats (28%) showed hindlimb weakness of varying degree (BBB score 0 to 18) immediately after the operation. Two rats died at 5 and 6 weeks, respectively, due to urinary retention, although their hindlimb weaknesses were improving. The recovery of motor weakness was observed until 5^{th} week and remained stationary thereafter (Figure 6). In 5 rats, the degree of motor weakness was not

equivalent in the two sides of the hindlimbs. Of the 5, the motor function of bilateral hindlimbs improved to a similar level in 2 whereas the difference remained despite overall improvement in 3.

Urinary retention was noted in 13 out of the 40 rats (33%) immediately after the operation. Although majority of them were mild retention, 10% showed severe dyssynergia of the urinary sphincter. The urinary function fully recovered within 2 weeks for 62% (8 / 13) of rats and took 2 weeks to 1 month for 38%. Of the delayed recovery group, 1 of the 5 rats eventually died due to urinary tract infection caused by prolonged urinary dysfunction.

Correlation between delayed mortality and neurologic status was assessed. Delayed mortality was far more frequent in rats with delayed urinary dysfunction (p-value = 0.009, Table 1).

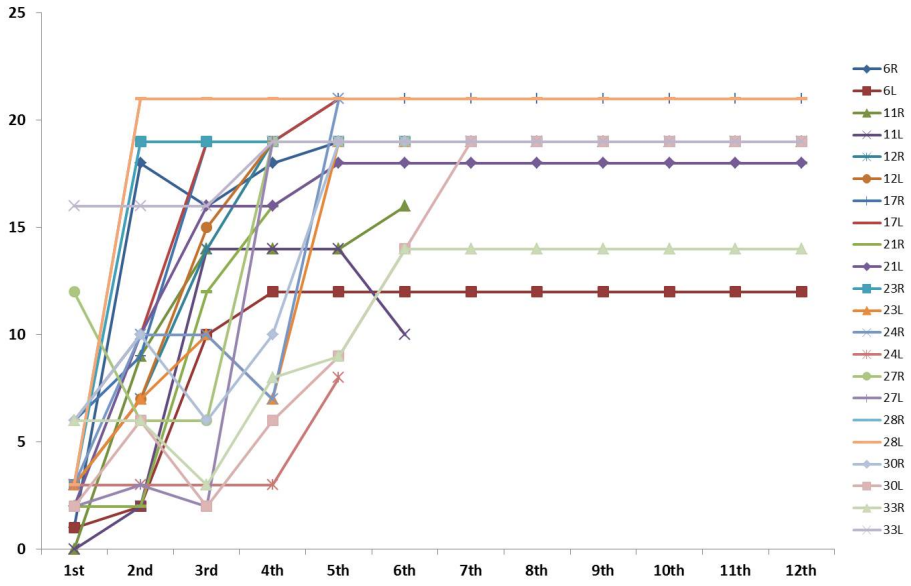

Figure 6. Plot of BBB scores

The weekly BBB scores of each hindlimb of rats that showed motor deficit were plotted. Most of the graphs came to plateau after the 5th week, meaning active recovery of the motor function is completed in this period.

Table 1 Correlation between delayed mortality and neurologic status

		Delayed mortality		
		Yes	No	p-value
Initial urinary dysfunction	Yes	1	12	0.469
	No	4	23	
Initial motor deficit	Yes	2	9	0.422
	No	3	26	
Delayed urinary dysfunction	Yes	3	0	0.009
	No	2	35	

MRI

Five out of 7 rats showed syringomyelia on the MRI. One rat did not show syringomyelia, and the other one was a sham-operated case.

Serial images of 1 rat revealed that syringomyelia was not evident until 2 months after the operation. Enlargement of the syrinx cavity was noted (Figure 7). In line with the H & E section data, largest diameter of the syringomyelia cavity appeared just cephalad to the compression site (Figure 8).

Whereas all the rats with prominent syringomyelia on the MRI had definite compression by the injected kaolin, the rat without evidence of syringomyelia had minimal compression (Figure 9).

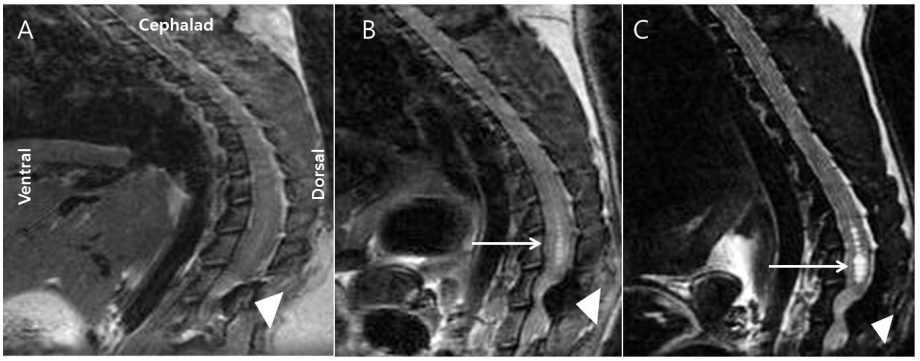

Figure 7. Syringomyelia in a rat: serial images

Serial sagittal T2 WI at (A) 1 month, (B) 2 months, and (C) 3 months after the operation showing the formation of syringomyelia (arrow) cephalad to the compression site (arrow head). Notice the syringomyelia appears at 2 month, and enlarges prominently at 3 month.

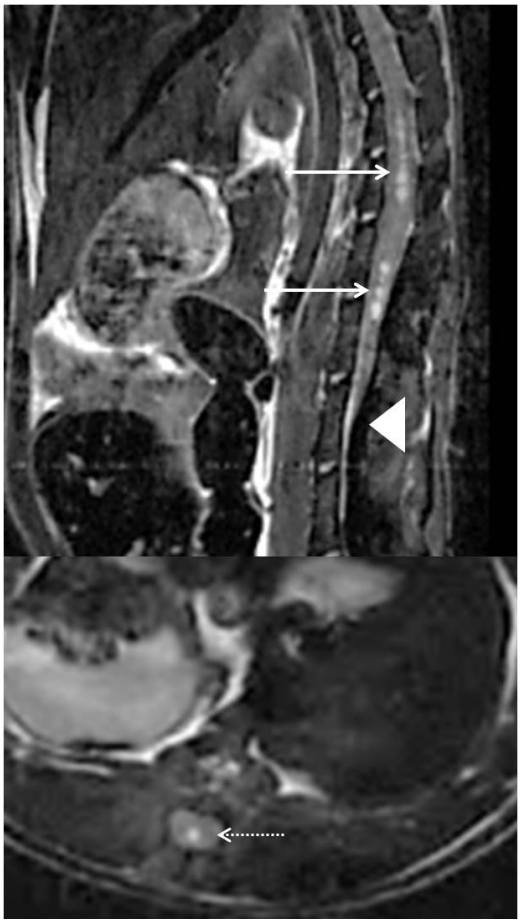

Figure 8. Syringomyelia in a rat

Another example of syringomyelia (arrows) shown at 3 months after the operation on sagittal (top) and axial (bottom) T2 WIs. Syrinx cavity is located cephalad to the compression site (arrow head). Syringomyelia is well-visualized in axial images (dotted arrow).

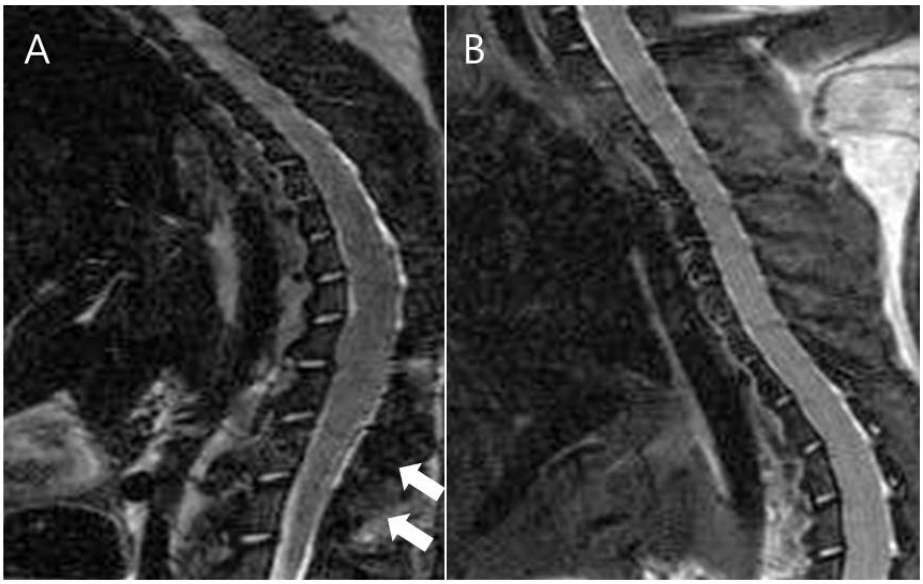

Figure 9. Rats with no syringomyelia on MRI

The rat with no evident syringomyelia on sagittal T2 WI (A) had very minimal compression on the spinal cord (injected kaolin denoted by the arrows), similar to the sham-operated control animal (B) implying that effective compression may be critical in the formation of syringomyelia in this animal model.

\Immunohistochemistry

After 12 weeks, 34 out of 40 rats (85%) showed enlargement of the central canal. The overall success rate of this model was 68% (34 / 50) including the early mortality cases, and 85% (34 / 40) excluding them. All of them consisted of true hydromyelia and no syringomyelia in the parenchyma were noted (Figure 10). The ependymal lining of the central canal was intact. The average central canal - cord ratio of the experimental group was 0.071 (SD: 0.017), whereas it was 0.008 (SD: 0.002) in the normal control group (p-value < 0.05). Few small cystic changes in the grey matter were seen which were not present in normal controls.

There was no significant increase in GFAP-immunoreactive astrocytes compared with sham-operated animals (Figure 11-B). NeuN staining showed similar number and distribution of neurons in experimental animals' grey matter compared with controls (Figure 11-C). No difference was found in the oligodendrocytes as shown by CC1 (Figure 11-D). Also, infiltration of macrophages or activation of resident central nervous system (CNS) microglia was not observed in the grey matter of experimental animals as shown in the ED1 staining (Figure 11-E). Slight increase of ED1 positive cells in the dorsal white matter was seen in some specimens, but the trend was not significant. Caspase-3 staining was done to check for apoptotic cell death, and positive cells were not different from the control animals (Figure 11-F). LFB staining revealed that there was no significant demyelination in the syringomyelia animals (Figure 11-G).

We found 2 samples where the kaolin was injected intradurally. These did

not have syringomyelia, but cystic changes in the grey and white matter were seen (Figure 11-A). Also, increased number of ED1 positive macrophages was seen near vessels of the white matter, suggesting breakdown of the blood-spinal cord barrier and infiltration of macrophages (Figure 11-E). Patchy demyelination was seen with LFB (Figure 11-G). The IHC results are summarized in Table 2.

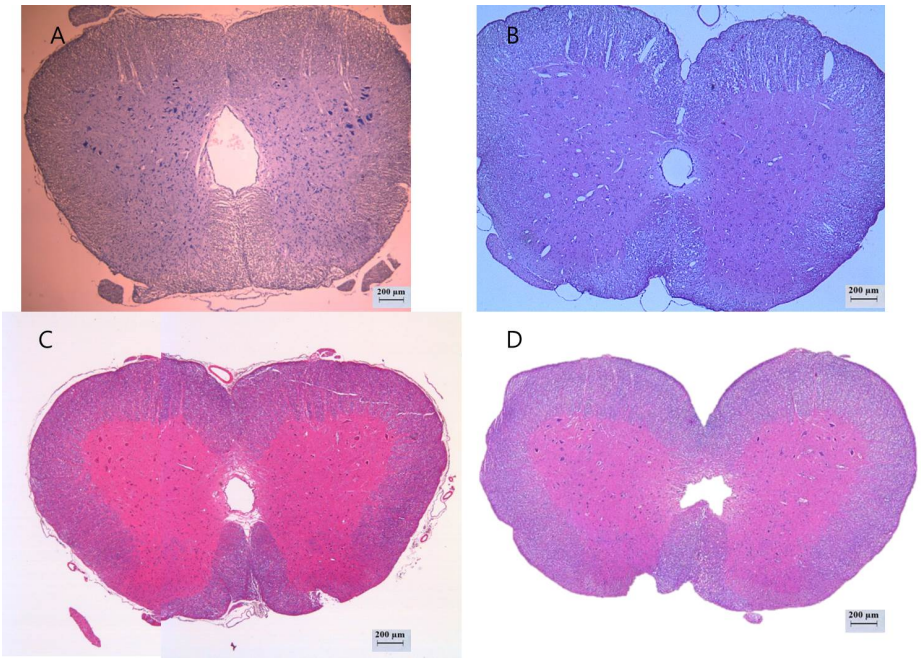

Figure 10. Histological confirmation of syringomyelia

Axial sections of 4 representative experimental rats' spinal cords show enlargement of central canal, forming syringomyelia (scale bar: 200μm)

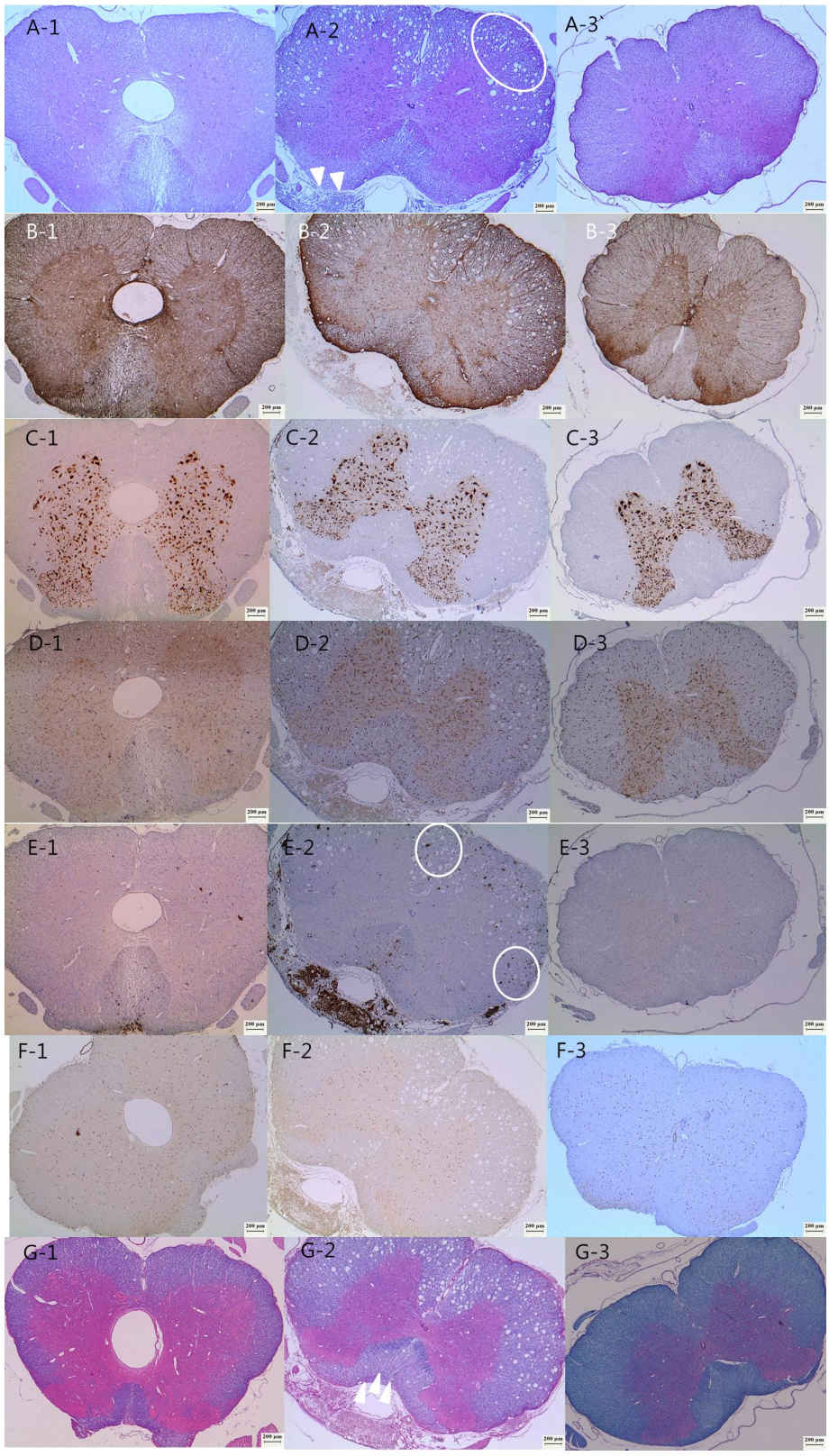
A-1
A-2
A-3
B-1
B-2
B-3
C-1
C-2
C-3
D-1
D-2
D-3
E-1
E-2
E-3
F-1
F-2
F-3
G-1
G-2
G-3

Figure 11. Comparison of immunohistochemistry between animal with epidural injection of kaolin, intradural injection of kaolin, and sham surgery

The first, second, and third columns are sections from a rat with epidural injection of kaolin (A ~ G – 1), intradural injection of kaolin (A ~ G – 2), and sham surgery (A ~ G – 3), respectively. Each rows are stainings of the following : (A) H & E (morphology), (B) GFAP (reactive astrocytes), (C) NeuN (neurons), (D) CC1 (oligodendrocytes), (E) ED1 (macrophage or microglia), (F) Caspase-3 (apoptosis), (G) LFB (demyelination). Scale bar: 200μm

Besides the clear enlargement of the central canal (syringomyelia) seen in A – 1, no difference is evident between the epidural injection group and the sham operation group (B ~ G – 1 vs B ~ G – 3).

H & E staining of intradural injection of kaolin (A-2, arrow heads) shows small central canal but extensive spongiform changes in the dorsal and ventral white matter (white circles). Also, much increased number of ED1 positive cells are seen throughout the white matter (E-2, white circles) compared to the sham operation (E-3), suggesting inflammatory process. Patchy demyelination (G-2, arrow heads) is also observed in the intradural injection sample.

Table 2 Comparison between epidural injection, intradural injection, and sham groups in IHC results

	Epidural injection (Syringomyelia)	**Intradural injection**	**Sham**
Morphology (H & E)	Enlarged central canal, otherwise normal	Spongiform changes in the white matter	normal
Extent of astrogliosis (GFAP)	No difference from sham	No difference from sham	Scanty GFAP positive astrocytes in the white and grey matter
Neuronal loss (NeuN)	No difference from sham	No difference from sham	Neurons in the grey matter
Oligodendrocyte (CC1)	No difference from sham	No difference from sham	Distributed throughout white and grey matter
Macrophage infiltration (ED1)	No difference from sham	Much increased in the white matter	Very few
Apoptosis (Caspase-3)	No difference from sham	No difference from sham	Scattered throughout the white and grey matter
Demyelination (LFB)	No difference from sham	Patchy demyelination	No demyelination

DISCUSSION

In this study, a novel rat model of syringomyelia by chronic epidural compression of the spinal cord using kaolin has been established. The main mechanism utilized to elicit syringomyelia was chronic compression for 12 weeks. Epidural location was chosen to eliminate the possibility of inflammatory reactions as caused by other syringomyelia models with intradural modulations (17). Early mortality rate was fairly high (20%, 10 out of 50) probably due to anesthesia, surgical procedure, or acute urinary retention. After 12 weeks, syringomyelia was detected in 85% of the animals (34 out of 40) as evident on the MRI and histologic examination. The syringes were usually found cephalad to the compression site. Initial dysfunctions of the hindlimb motor (11 out of 40, 28%) and lower urinary tract (13 out of 40, 33%) were seen. On histologic examination, dilatation of the central canal was observed exclusively, and there were no cases of intramedullary syringomyelia. IHC revealed no evidence of inflammatory reaction or demyelination, suggesting the core mechanism of syringomyelia was not inflammation or decreased blood flow but physical compression of the cord. Unexpected delayed mortality was seen in 5 rats, 3 of which were probably due to the suddenly developed neurogenic bladder.

Comparison with other noncommunicating syringomyelia models

This model seems to be unique compared with other noncommunicating syringomyelia models. First, previous models for noncommunicating

syringomyelia universally show the involvement of inflammation as one of the main mechanisms of syrinx formation (10, 18, 19). In one study, subarachnoid injection of low concentration of kaolin in the lumbar spine of rats revealed infiltration of reactive lymphocytes and formation of syringomyelia unrelated to the central canal (20). The authors concluded that syringomyelia was formed as a result of intramedullary degeneration in association with arachnoiditis. Despite the similarity in lesion location and injected material, their model is quite different from ours; extensive damage of the white matter with lymphocyte infiltration and intact central canal were found. A recent study that combined the two representative etiologies of noncommunicating syringomyelia, trauma and arachnoiditis also revealed extensive macrophage / microglial-associated inflammation and astrogliosis at the lesion (14).

Interestingly, there were two samples of which intradural injection of the kaolin was done in our study. Both of these ‘unexpected’ control group rats showed far more ED1 positive cells in the white matter and more pronounced demyelination. Spongy changes in the white matter were also profound compared to the epidural injection group. The ‘internal’ comparison between the epidural and intradural injection group also implies that the relatively limited extent of reactive inflammation and demyelination seen in the epidural injection group may be due to the epidural location of the compression.

Second, it should be noted that the present model exclusively showed dilatation of the central canal and no cystic dilatation in the parenchyma. In other words, the model produced pure hydromyelias. This is different from

most of the noncommunicating syringomyelia models which showed hydromyelia as well as intramedullary syringomyelia (10, 14, 21).

Last, the time of formation of the syrinx is more delayed in the present study, thereby making it a “chronic” model of syringomyelia. Majority of the noncommunicating syringomyelia models show acute syringomyelia formation starting within a period of several days and progress until 6 weeks.

Comparison with other spinal cord compression models

There have been other models of spinal cord compression, and methods such as tumor cell implantation (22, 23), tightening of screws (24, 25), insertion of plastic sheets (26) or rubber (27), and inflation of balloons (28) were used. These models could be categorized by onset and duration of compression. A tumor cell implantation model is slow or chronic in the onset of compression because it takes 10 to 20 days for the tumor to grow and cause compression of the cord. A balloon inflation model would cause rapid or acute onset of compression. The present model also is ‘acute’ in terms of onset of compression because the kaolin material changed from paste to solid within an hour. Regarding the duration of compression, in previous models of balloon inflations or plastic sheet insertions, the compression was kept for a few hours to not more than a few days. These models used short or acute duration of compression. More prolonged or chronic duration of compression up to 25 weeks was achieved in more recent studies. The present study, with 12 weeks of compression, may be categorized as a prolonged, chronic compression group. However, regardless of the type of onset or duration of

compression, none of the previous compression models has observed syringomyelia on histologic examination.

One recent study in particular, which was similar to the present model with acute onset and chronic duration of compression, should be noted (26). As a model for cervical myelopathy, epidural compression at the cervical vertebra levels 5 and 6 by a thin sheet of expanding polymer was performed. The rats were observed up to 25 weeks with no evidence of inflammation or demyelination on histologic examination which is in accordance with our results. However, syringomyelia was not found in their model. The H & E photographs showed no enlargement of the central canal. The reason for this contradictory result in syringomyelia formation despite the similarity in other aspects can only be speculated. The most obvious difference between the abovementioned and our model is the location of the compression, cervical and lumbar, respectively. The fluid dynamics in the spinal canal and spinal cord may be influenced by the distance from the craniovertebral junction, which may have brought about the contrasting result. Also, whereas rats aged 5 to 6 weeks were used in the present study, the abovementioned study used those of 12 to 14 weeks and the age difference may herald some variation in the fluid dynamics of the spinal cord. However, further studies are needed to elucidate the mechanism.

Comparison with spinal cord injury models

In terms of motor and lower urinary tract dysfunction, interpretation in comparison to the SCI models is only available, because functional outcome

is usually not dealt in detail in syringomyelia models. First, the number of rats with dysfunctions is relatively low compared to other models, because in SCI models, deficits are seen in majority of rats and mostly within certain range (14, 29). Second, the time and extent of recovery are different in this study. Whereas in usual SCI, it takes 6 weeks in average for motor and urinary tract recovery, in the present model, rats recovered their urinary function in 2 weeks, and the motor deficits took 5 weeks in average. Third, the final outcome was also better in our study than others. We think this reflects the chronic, mild compressive nature of this model. Lastly, delayed onset new neurologic deficit observed in our study is noteworthy. Of the rats which died unexpectedly 1 month or more after the operation, 3 of them had no deficits initially but had neurogenic bladder of new onset. Although due to their almost sudden death, it was not possible to check the MRI or sacrifice the animal for spinal cord specimen, we think that gradual formation of the syringomyelia may have caused the delayed onset of new neurological problems. This shows the possibility of using this model to assess the neurologic symptoms and signs of syringomyelia. Such behavioral aspects are clinically important, but in syringomyelia animal models, the experiments have been focused in the pathogenesis.

Pathogenetic mechanism of syringomyelia formation

Multiple hypotheses have been postulated regarding the pathogenetic mechanism of syringomyelia associated with different conditions. Most classic hypothesis is the ‘water-hammer theory’ proposed by Gardner (30),

followed by William's 'suck effect theory' (31) and Oldfield's 'piston theory' (32). However, these concepts are focused on the pathophysiology of Chiari associated syringomyelia. Recently a 'unified' theory of 'intramedullary pressure' has been proposed to provide an explanation for the pathophysiology of syringomyelia regardless of underlying etiology (1). The authors state that the syringomyelia is formed by distension of the cord and the progressive accumulation of the extracellular fluid. Distension of the cord is brought about by a relative increase in the pulse pressure in the spinal cord compared to that of the cerebrospinal fluid (CSF) pulse pressure in the nearby subarachnoid space, and also by the "Bernoulli theorem" which causes the decrease in CSF pulse pressure in the narrowed subarachnoid space. The intramedullary pulse pressure theory applies well for Chiari malformation (dynamic and partial obstruction at the foramen magnum) and posttraumatic condition (fixed and partial or total impediment at any segment of the spinal cord). The present model may be seen as a model of fixed and total obstruction of subarachnoid space in a fairly long segment of the spinal cord, most similar to the case of spinal tumors. However, because the CSF pulse pressure originates from the pressure wave of CSF displaced from the head during arterial pulsations, "the compliance of the thecal sac decreases the systolic pulse wave as it propagates down the spinal canal". Therefore, in the case of spine tethering at more caudal regions, the authors suggest flexion movement to be an additional cause of mechanical distension and traction of the spinal cord. Still, as discussed earlier about contrasting results in syringomyelia formation in the chronic epidural compression of cervical and

lumbar regions, unrevealed differences in the fluid dynamics according to the proximity to the craniocervical junction may be playing a critical role in the pathophysiology of syringomyelia in the present model. Therefore, further elucidation of the pathogenetic mechanism of the present animal model may reveal other specific elements of syringomyelia.

Association with occult spinal dysraphism

Ideally, the clinical relevance of studies using an animal model would be optimized if the disease model recapitulated events known to play a pathogenetic role in the clinical disease. From clinical observations, cord tethering may be the most important pathologic mechanism underlying lumbosacral lipomas and other occult spinal dysraphism. However, constructing a tethering model in rat was technically not feasible because the spinal cord and filum terminale was very fragile. Therefore, this study focused on and attempted to recapitulate one aspect of the pathology of lumbosacral lipoma, a chronic, mechanical compression of spinal cord. A previous study has recapitulated the tethering effect by applying 5.0 grams of traction for 10 minutes to filum terminale of guinea pigs then fixating the filum to the sacrum using cyanoacrylate (33). Evaluation of electrophysiological properties and morphology using transmission electron microscope was done 10 days after the surgical procedures. Defective conduction in the motor and sensorial nerve fibers were proven as well as edema, destruction of grey-white matter junction, scarcity of neurofilaments, destruction in axons, and damage in

myelin sheath. However, syringomyelia was not observed, possibly because it was an acute model.

Limitations and future directions

There are several limitations of this study. First, as mentioned above, although the study evolved from the need of an animal model of syringomyelia associated with lumbosacral occult spinal dysraphism, it only partially resembles the etiological condition. Only the compressive mass effect on the spinal cord is recapitulated, lacking the tethering component. Furthermore, epidural location of the compression does not match the intradural location of lumbosacral lipomas, and rather shows location-wise similarity to epidural tumors or spinal stenosis. Second, the fact that symptomatic deterioration to correlate with the gradual formation of syringomyelia was not observed is puzzling. A more detailed evaluation of the neurologic status, such as a more thorough, quantitative assessment of urinary function and additional evaluation of sensory function of the rats, with longer observation periods may have potentially detected subtle changes in neurologic status, if any. Third, relatively low success rate should be noted. The experiment enrolled a total of 50 animals and the final yield was 34 animals, giving a success rate of 68%. The biggest problem was the high early mortality of 20%, which may be corrected by improvement in anesthesia and immediate postoperative care. Also, technical variations especially regarding adequate compression may have caused failure. As shown in the MRI scans, a

small portion of the rats may not have effective compression, resulting in failure of syringomyelia formation.

Further studies with epidural compression in the thoracic or cervical level may elucidate the mechanism underlying syringomyelia formation in this model. Also, application of various therapeutic means such as decompressive surgery is mandatory.

CONCLUSION

A novel animal model of syringomyelia by epidural compression of the lumbosacral spinal cord using highly concentrated kaolin for 12 weeks was established. The exclusive enlargement of central canal, cephalad to the compression site was observed on histologic examination and MRI. No evidence of inflammation in the spinal cord with syringomyelia was found in IHC studies, clearly differentiating the present model from previous models of noncommunicating syringomyelia. Further studies on the pathogenetic mechanism and therapeutic strategies of the established model will be interesting.

REFERENCES

1. Greitz D. Unraveling the riddle of syringomyelia. Neurosurg Rev. 2006;29(4):251-63; discussion 64.

2. Iskandar BJ, Oakes WJ, McLaughlin C, Osumi AK, Tien RD. Terminal syringohydromyelia and occult spinal dysraphism. J Neurosurg. 1994;81(4):513-9.

3. Koyanagi I, Iwasaki Y, Hida K, Abe H, Isu T, Akino M. Surgical treatment of syringomyelia associated with spinal dysraphism. Childs Nerv Syst. 1997;13(4):194-200.

4. Lee JY, Phi JH, Cheon JE, Kim SK, Kim IO, Cho BK, et al. Preuntethering and postuntethering courses of syringomyelia associated with tethered spinal cord. Neurosurgery. 2012;71(1):23-9.

5. Brodbelt AR, Stoodley MA, Watling A, Rogan C, Tu J, Brown CJ, et al. The role of excitotoxic injury in post-traumatic syringomyelia. Journal of neurotrauma. 2003;20(9):883-93.

6. Chakrabortty S, Tamaki N, Ehara K, Ide C. Experimental syringomyelia in the rabbit: an ultrastructural study of the spinal cord tissue. Neurosurgery. 1994;35(6):1112-20.

7. Chang HS, Nakagawa H. Theoretical analysis of the pathophysiology of syringomyelia associated with adhesive arachnoiditis. J Neurol Neurosurg Psychiatry. 2004;75(5):754-7.

8. Cho KH, Iwasaki Y, Imamura H, Hida K, Abe H. Experimental model of posttraumatic syringomyelia: the role of adhesive arachnoiditis in syrinx formation. J Neurosurg. 1994;80(1):133-9.

9. Cohen WA, Young W, DeCrescito V, Horii S, Kricheff, II. Posttraumatic syrinx formation: experimental study. AJNR Am J Neuroradiol. 1985;6(5):823-7.

10. Milhorat TH, Nobandegani F, Miller JI, Rao C. Noncommunicating syringomyelia following occlusion of central canal in rats. Experimental model and histological findings. J Neurosurg. 1993;78(2):274-9.

11. Stoodley MA, Gutschmidt B, Jones NR. Cerebrospinal fluid flow in an animal model of noncommunicating syringomyelia. Neurosurgery. 1999;44(5):1065-75; discussion 75-6.

12. Yang L, Jones NR, Stoodley MA, Blumbergs PC, Brown CJ. Excitotoxic model of post-traumatic syringomyelia in the rat. Spine. 2001;26(17):1842-9.

13. Schwartz ED, Yezierski RP, Pattany PM, Quencer RM, Weaver RG. Diffusion-weighted MR imaging in a rat model of syringomyelia after excitotoxic spinal cord injury. AJNR Am J Neuroradiol. 1999;20(8):1422-8.

14. Seki T, Fehlings MG. Mechanistic insights into posttraumatic syringomyelia based on a novel in vivo animal model. Laboratory investigation. J Neurosurg Spine. 2008;8(4):365-75.

15. Stoodley MA, Jones NR, Yang L, Brown CJ. Mechanisms underlying the formation and enlargement of noncommunicating syringomyelia: experimental studies. Neurosurg Focus. 2000;8(3):E2.

16. Basso DM, Beattie MS, Bresnahan JC. A sensitive and reliable locomotor rating scale for open field testing in rats. Journal of neurotrauma. 1995;12(1):1-21.

17. Pang D, Zovickian J, Oviedo A. Long-term outcome of total and near-total resection of spinal cord lipomas and radical reconstruction of the neural placode: part I-surgical technique. Neurosurgery. 2009;65(3):511-28; discussion 28-9.

18. Milhorat TH, Adler DE, Heger IM, Miller JI, Hollenberg-Sher JR. Histopathology of experimental hematomyelia. J Neurosurg. 1991;75(6):911-5.

19. Williams B, Bentley J. Experimental communicating syringomyelia in dogs after cisternal kaolin injection. Part 1. Morphology. Journal of the neurological sciences. 1980;48(1):93-107.

20. Tamaki N, Nagashima T. [Hydrodynamics of syringomyelia]. Rinsho shinkeigaku = Clinical neurology. 1995;35(12):1398-9.

21. Kobayashi S, Kato K, Rodriguez Guerrero A, Baba H, Yoshizawa H. Experimental syringohydromyelia induced by adhesive arachnoiditis in the rabbit: changes in the blood–spinal cord barrier, neuroinflammatory foci, and syrinx formation. Journal of neurotrauma. 2012;29(9):1803–16.

22. Delattre JY, Arbit E, Thaler HT, Rosenblum MK, Posner JB. A dose–response study of dexamethasone in a model of spinal cord compression caused by epidural tumor. J Neurosurg. 1989;70(6):920–5.

23. Manabe S, Tanaka H, Higo Y, Park P, Ohno T, Tateishi A. Experimental analysis of the spinal cord compressed by spinal metastasis. Spine. 1989;14(12):1308–15.

24. al–Mefty O, Harkey HL, Marawi I, Haines DE, Peeler DF, Wilner HI, et al. Experimental chronic compressive cervical

myelopathy. J Neurosurg. 1993;79(4):550-61.

25. Shinomiya K, Mutoh N, Furuya K. Study of experimental cervical spondylotic myelopathy. Spine. 1992;17(10 Suppl):S383-7.

26. Kim P, Haisa T, Kawamoto T, Kirino T, Wakai S. Delayed myelopathy induced by chronic compression in the rat spinal cord. Ann Neurol. 2004;55(4):503-11.

27. Sekiguchi M, Kikuchi S, Myers RR. Experimental spinal stenosis: relationship between degree of cauda equina compression, neuropathology, and pain. Spine. 2004;29(10):1105-11.

28. Konno S, Yabuki S, Sato K, Olmarker K, Kikuchi S. A model for acute, chronic, and delayed graded compression of the dog cauda

equina. Presentation of the gross, microscopic, and vascular anatomy of the dog cauda equina and accuracy in pressure transmission of the compression model. Spine. 1995;20(24):2758-64.

29. Ozsoy O, Ozsoy U, Stein G, Semler O, Skouras E, Schempf G, et al. Functional deficits and morphological changes in the neurogenic bladder match the severity of spinal cord compression. Restorative neurology and neuroscience. 2012;30(5):363-81.

30. Gardner WJ, Goodall RJ. The surgical treatment of Arnold-Chiari malformation in adults; an explanation of its mechanism and importance of encephalography in diagnosis. J Neurosurg. 1950;7(3):199-206.

31. Williams B. Cerebrospinal fluid pressure changes in response to coughing. Brain : a journal of neurology. 1976;99(2):331-46.

32. Oldfield EH, Muraszko K, Shawker TH, Patronas NJ. Pathophysiology of syringomyelia associated with Chiari I malformation of the cerebellar tonsils. Implications for diagnosis and treatment. J Neurosurg. 1994;80(1):3-15.

33. Kocak A, Kilic A, Nurlu G, Konan A, Kilinc K, Cirak B, et al. A new model for tethered cord syndrome: a biochemical, electrophysiological, and electron microscopic study. Pediatr Neurosurg. 1997;26(3):120-6.

국문 초록

서론:

현재 잠재성 척추이형성증과 동반되는 척수공동증에 대한 동물 모델이 없다. 척추공동증에 대한 기존 연구가 대부분 키아리 기형, 외상, 혹은 염증에 의한 것이 대부분이기 때문이다. 이에 본 연구는 잠재성 척추이형성증에서 나타나는 척수공동증의 발생기전에 대한 연구의 일환으로, 요천추부 척수에 대한 만성적 압박을 통해 새로운 척수공동증 동물 모델을 개발하고자 하였다.

방법:

새로운 동물 모델 개발을 위해 Sprague-Dawley 랫드 (40 마리)를 이용하였다. 요추 1 번과 요추 5 번에서 부분 후궁절제술을 하고, 높은 농도의 kaolin 반죽을 경막외로 주입하여 12 주간 유지하였다. 그 기간 동안 동물들의 행동/기능적인 결과를 추적하였고, 자기공명영상을 이용하여 척수공동증의 형성을 확인하였다. 12 주 후에 조직에 대한 형태학적 분석을 통해 척수공동증을 확인하였고, 또한 다양한 면역염색 검사를 통해 염증반응, 탈수초화 및 세포 사멸의 정도를 평가하였다.

결과:

약 28% (11 / 40)의 동물에서 수술 직후 다양한 정도의 운동 마비가 보였고, 33% (13 / 40)에서는 하부요로계의 기능 이상이 확인되었다. 운동 마비의 경우 수술 후 5 주까지 회복이 관찰되었고, 소변 기능의 경우 대다수에서 2 주내에 회복이 관찰되었다. 수술 후 한달 이후에 개체 사망은 5 마리에서 관찰되었는데, 특히 이 중 60%의 경우는 새로 발생한 하부요로계 기능 이상에 의한 사망임을 주목할 만 하다. MRI 에서 확실한 척수공동증은 수술 후 8 주째부터 관찰되었고, 척수공동증은 압박 부위의 바로 위쪽에 발생하였다. 12 주에 조직에서 확인하였을 때 85% (34 / 40)의 랫드에서 척수공동증이 형성되어 있었다. 면역염색에서 정상에 비해 염증이나 탈수초화 정도에는 큰 차이가 없었다.

결론:

본 연구를 통해 요천추부 척수에 대한 경막외 압박에 의해 발생하는 척수공동증에 대한 최초의 동물 모델을 확립하였다. 이는 향후 척수공동증의 병태 생리 연구에 중요한 도구로 사용될 수 있을 것이며, 나아가 이를 통해 요추부 척수강내의 뇌척수액 수액동역학에 대한 연구의 새 지평이 열리는 것도 기대해 볼 수 있겠다.

주요어 : 척수공동증, 잠재성 척추이형성증, 요척추지방종, 뇌척수액
수액동역학, 척수 실질
학 번 : 2011-30612

감사의 글

부족한 저를 긴 석사 및 박사 기간 동안 지도해주시고, 매사에 격려해주신 저의 지도교수님이신 백선하 교수님께 감사의 인사 올립니다. 또한 연구 전반에 걸쳐 조언을 해주시고 이끌어주신 왕규창 교수님께도 감사의 말씀 올립니다. 바쁘신 중에도 제 논문을 꼼꼼히 심사해주신 김기중 심사위원장님과 천정은, 심기범 심사위원 교수님들께도 깊은 감사 드립니다. 또한 본 연구의 진행에 중추적인 역할을 한 김샛별, 김신원 연구원께도 고마운 마음을 전합니다.

저의 학문적 능력을 양성해주시고, 의사로서의 됨됨이를 가르쳐주신 스승님들이신 조병규, 왕규창, 김승기 교수님께도 미미하지만 학위 논문을 통해 감사의 뜻을 전해드리고자 합니다.

언제나 인내심으로 저를 아껴주고 응원해주는 남편에게 감사드립니다. 마지막으로, 저의 모든 능력을 주시고, 36년 동안 한결같이 저를 키워주신 부모님께 사랑과 감사를 드리고, 박사 학위 논문을 바칩니다.